On Velocity Estimation and Correlation Properties of Narrow-Band Mobile Communication Channels

Cihan Tepedelenlioğlu and Georgios B. Giannakis, *Fellow, IEEE*

***Abstract*—Estimation of the maximum Doppler spread or, equivalently, the vehicle velocity, is useful in improving handoff algorithms and necessary for the optimal tuning of parameters for systems that adapt to changing channel conditions. We provide a novel velocity estimator based on the spectral moments of the in-phase and the quadrature phase components or the envelope of the received signal. We characterize the joint effects of the Ricean K factor, the directivity and the angle of nonisotropic scattering, and the effects of additive white noise on our estimator and other covariance-based velocity estimators analytically. We also prove the mean-square consistency of the covariance-based velocity estimators under some assumptions on the angle of arrival distribution. Simulations illustrate our approach and compare with existing techniques.**

***Index Terms*—Fading channel models, velocity estimation.**

I. Introduction

In mobile communication systems, the received signal strength varies significantly in space due to constructive and destructive interference arising due to multipath components, a phenomenon also known as small scale fading [18]. The mobile velocity dictates how fast in time the fading is experienced by the receiver, and its knowledge at the base station can be utilized for handoff purposes. This is because the average signal strength is often the parameter that dictates handoff and its accurate but quick estimation introduces a tradeoff that necessitates the appropriate choice of a temporal averaging window length, which, in turn, is dependent on the mobile velocity [5]. The base stations' knowledge of the vehicle velocity is also useful in overlaid cell architectures where slow mobiles are assigned to microcells and fast ones to "umbrella" macrocells.

The mobile velocity v is proportional to the maximum Doppler spread ω_D through $\omega_D = (2\pi v f_c)/c$, where f_c is the carrier frequency and c is the speed of propagation. Hence, given the system parameters, estimating v and estimating ω_D are equivalent. In many communication applications such as adaptive coding/modulation/antenna diversity/power control, knowledge of ω_D is of paramount importance in adapting the system parameters to new channel conditions [12], [6]. In fact, when the angle-of-arrival (AOA) distribution is uniform and a line-of-sight (LOS) component is absent, ω_D is the sole parameter that determines the Doppler spectrum [13]. But as the need for higher spectral efficiency increases, directional antennas are used to avoid interference, making it necessary to characterize the effects of the LOS component and directional scattering on velocity estimators.

In this paper, in addition to proposing novel velocity (Doppler) estimators, we characterize analytically, the robustness of existing velocity estimators [level crossing rate (LCR)-based as well as covariance-based] to nonuniform AOA distributions and the presence of a LOS component. Utilizing an intuitively appealing model, we prove the mean-square consistency of the in-phase and quadrature-phase (I/Q) components' sample covariances under certain assumptions on the AOA distribution, which establishes the consistency of the covariance-based estimators that rely on the I/Q components. As a byproduct of this derivation, we generalize Aulin's result [4] for the covariance of the squared envelope to when the I/Q components are correlated with each other. Using this result, we also show that the moment-based method to estimate the Ricean K-factor in [7] is useful even when the LOS component is not perpendicular to the direction of the mobile, hence (sinusoidally) time varying. We illustrate by simulation that when the sampling rate is high and the estimation window is small, the covariance-based estimators have significantly smaller sample variances than their LCR-based counterparts, and show that among the covariance-based estimators, the proposed method has the least sample variance in this regime.

In Section II, we provide a parametric model for the AOA distribution, by using the von Mises probability density function (pdf), also used in [1], [2], and provide the resulting correlation function, Doppler spectrum, LCR, and the covariance of the squared envelope as a function of the parameters of this pdf and the Ricean K-factor. In Section III we introduce the proposed velocity estimator and in Section IV we delineate its relationship with other covariance-based estimators. In Section V, we derive the joint effect of the LOS factor, scattering directivity and their angles of arrival, on the covariance-based velocity estimators. Section VI briefly outlines estimation of the Ricean K factor and Section VII analyzes the effect of additive white noise on covariance-based velocity estimators. In Section VIII, simulations illustrate the results.

A few words on notation. We will use * for conjugate, $\angle$ for phase, $\mathcal{R}\{\cdot\}$ for real part, and $\mathcal{I}\{\cdot\}$ for imaginary part of a complex number; $E[\cdot]$ will denote mathematical expectation with respect to all the random variables within the brackets; $\delta_K[n]$ and $\delta_D(t)$ denote the Krönecker's delta function and Dirac's delta

Manuscript received March 3, 2000; revised January 5, 2001. This work was supported by ARO Grant DAAG55-98-1-0336, ARL Grant 7850-98, and the NSF Wireless Initiative Grant 9979443. Part of the results in this paper appeared in *Proceedings of the 34th Conference on Information Sciences and Systems (CISS)*, March 2000, and *Proceedings of the Wireless Communication and Networking Conference (WCNC)*, September 2000.

The authors are with the Department of Electrical and Computer Engineering, University of Minnesota, Minneapolis, MN 55455 USA (e-mail: georgios@ece.umn.edu; cihan@ece.umn.edu).

Publisher Item Identifier S 0018-9545(01)04888-5.

function, respectively; Superscript (n) will denote nth derivative, but if $n = 1$ or 2, we will also use $'$ or $''$, respectively; $\log(\cdot)$ denotes base 10 logarithm; for a generic complex, stationary stochastic process $x(t)$, we use $r_x(\tau) := E[x(t)x^*(t+\tau)]$ to denote its correlation function, and reserve $c_x(\tau) := r_x(\tau) - |E[x(t)]|^2$ for the covariance function at lag τ.

II. Channel Model

We will assume that the complex envelope of the narrow band (NB) randomly time-varying channel impulse response process in base-band $h(t)$ is given as the sum of a diffuse component $x(t)$ and a specular component $y(t)$

$$\begin{aligned} h(t) &= x(t) + y(t), \\ x(t) &= \frac{\sigma_h}{\sqrt{K+1}} \lim_{M\to\infty} \frac{1}{\sqrt{M}} \sum_{m=1}^{M} a_m e^{j(\omega_D \cos(\theta_m)t + \phi_m)} \\ y(t) &= \sigma_h \sqrt{\frac{K}{K+1}}\, e^{j(\omega_D \cos(\theta_0)t + \phi_0)} \end{aligned} \tag{1}$$

where

- θ_m, $m = 1, \ldots, M$: independent and identically distributed (i.i.d.) angles that the incoming waves make with the mobile direction, with density functions given by $p(\theta)$;
- ϕ_m: i.i.d. phases, uniformly distributed on $(-\pi, \pi]$;
- θ_0 and ϕ_0: *deterministic* constants;
- K: the Ricean factor, which is the ratio of the specular component $y(t)$s power to the diffuse component $x(t)$'s power;
- θ_0: the angle that the LOS component makes with the mobile direction;
- $\sigma_h^2 := E|h(t)|^2$: the power of the received signal;
- a_m: deterministic complex constants normalized to satisfy $\lim_{M\to\infty} M^{-1} \sum_{m=1}^{M} |a_m|^2 = 1$, so that $\sigma_h^2 = E|h(t)|^2$ holds.

Note that making M arbitrarily large ensures $x(t)$ to be a Gaussian process due to the central limit theorem, resulting in $|h(t)|$ being Ricean distributed. In the absence of a LOS component ($K = 0$), $|h(t)|$ has a Rayleigh density. Because the phases ϕ_m are uniformly distributed on $(-\pi, \pi]$, $E[x(t)] = 0$ and, hence, $E[h(t)] = y(t)$. Notice that $y(t)$ depends on time if the LOS component is not perpendicular to the direction of motion ($\theta_0 \neq \pi/2$); hence, similar to [4] and [16], we allow for a sinusoidally time varying specular component.

It follows from (1) that the correlation function of $h(t)$ is given by

$$\begin{aligned} r_h(\tau) &:= E[h(t)h^*(t+\tau)] \\ &= \frac{\sigma_h^2}{K+1} \int_{-\pi}^{\pi} p(\theta) e^{-j\omega_D \cos(\theta)\tau}\, d\theta \\ &\quad + \frac{K\sigma_h^2}{K+1} e^{-j\omega_D \cos(\theta_0)\tau} \end{aligned} \tag{2}$$

by direct substitution and using the assumptions on ϕ_m, θ_m and a_m.

We see from (2) that $r_h(\tau)$ depends on the probability distribution of the angle of arrival $p(\theta)$. In order to capture the effects of directional scattering on $r_h(\tau)$ in a parametric fashion will use the von Mises/Tikhonov distribution [15], [19]

$$p(\theta) = \frac{1}{2\pi I_0(\kappa)} e^{\kappa \cos(\theta - \alpha)}, \qquad \theta \in (-\pi, \pi] \tag{3}$$

where

- $I_n(\kappa)$: the nth order modified Bessel function of the first kind;
- κ: the beamwidth;
- α: the angle that the average scattering direction makes with the mobile direction.

Fig. 1 illustrates the von Mises distribution for different values of κ and $\alpha = 0$ [notice that $\kappa = 0$ reduces (3) to a uniform distribution and that an $\alpha \neq 0$ will merely rotate the plot by α radians]. The von Mises distribution is widely used in directional statistics [15] and has been justified empirically to be an accurate model for the AOA distribution for NB channels [2]. In addition, the von Mises pdf enables us to relate, in closed form, the effect of $\boldsymbol{\psi} := [K,\ \theta_0,\ \kappa,\ \alpha]$ to the Doppler spectrum, the correlation function and $r_h^{(n)}(0)$ [2]. Since many velocity estimators that rely on the covariance as well as those that rely on LCR's can be expressed as a function of $r_h^{(n)}(0)$, $n = 0, 1, 2$, we will use the closed-form expressions relating $\boldsymbol{\psi}$ to $r_h^{(n)}(0)$ in evaluating how velocity estimators designed assuming[1] $\boldsymbol{\psi} = \mathbf{0}$ are affected in environments for which $\boldsymbol{\psi} \neq \mathbf{0}$. In what follows, we will, in part, extend the results in [2] to when a LOS is present ($K \neq 0$).

Substituting (3) into (2) we see that the correlation function is given by

$$\begin{aligned} r_h(\tau) &= \frac{\sigma_h^2}{K+1} \frac{J_0\left(\sqrt{-\kappa^2 + \omega_D^2\tau^2 - 2j\kappa\cos(\alpha)\omega_D\tau}\right)}{I_0(\kappa)} \\ &\quad + \frac{K\sigma_h^2}{K+1} e^{-j\omega_D \cos(\theta_0)\tau} \end{aligned} \tag{4}$$

where $J_0(\cdot)$ is the zeroth-order Bessel function of the first kind. Notice that (4) is complex valued in general, but it is real when $K = \kappa = 0$, yielding $r_h(\tau) = \sigma_h^2 J_0(\omega_D\tau)$, the correlation function corresponding to Jakes's model [13].

The Doppler spectrum $S(\omega)$ is the Fourier transform of (2). Using the following relationship between the spectrum $S(\omega)$ and the density function $p(\theta)$ of θ_m, $S(\omega) = [p(\cos^{-1}(\omega/\omega_D)) + p(-\cos^{-1}(\omega/\omega_D))][1 - (\omega/\omega_D)^2]^{-1/2}$, we obtain a closed-form expression for $S(\omega)$ as a function of the directivity κ and the angle α

$$\begin{aligned} S(\omega) &= \frac{\sigma_h^2}{K+1} \frac{e^{\kappa\cos(\alpha)(\omega/\omega_D)} \cosh\left[\kappa \sin(\alpha)\sqrt{1 - \left(\frac{\omega}{\omega_D}\right)^2}\right]}{\pi I_0(\kappa)\sqrt{1 - \left(\frac{\omega}{\omega_D}\right)^2}} \\ &\quad + \frac{K\sigma_h^2}{K+1} \delta_D(\omega - \cos(\theta_0)). \end{aligned} \tag{5}$$

[1]Note that $\boldsymbol{\psi} = \mathbf{0}$ implies uniform AOA with no LOS component.

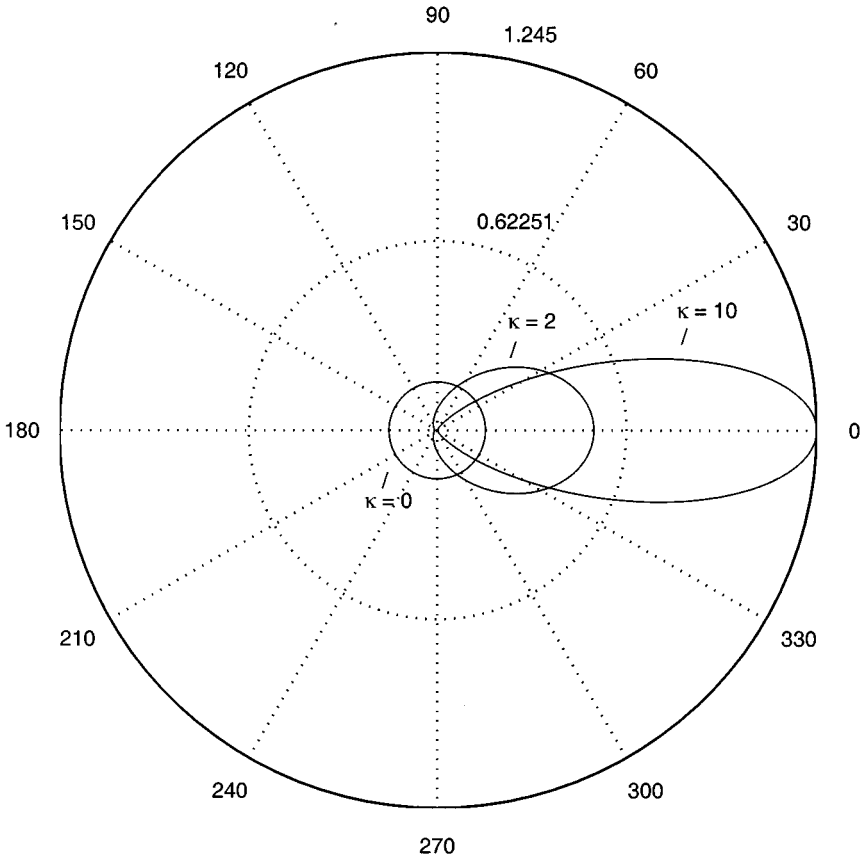

Fig. 1. The von Mises pdf.

Notice that (5) also reduces to Jakes's "U-shaped" spectrum [13] when $\boldsymbol{\psi} = \mathbf{0}$. In this case we have $S(\omega) = \sigma_h^2 \pi^{-1}[1 - (w/\omega_D)^2]^{-1/2}$.

The derivatives of the correlation function of the diffuse component at zero $r_x^{(n)}(0)$ play an important part in estimating ω_D. They can be derived using (2) and (3) as

$$r_x(0) = \frac{\sigma_h^2}{K+1} \tag{6}$$

$$r_x'(0) = -j\omega_D \frac{\sigma_h^2}{K+1}\left(\frac{\cos(\alpha) I_1(\kappa)}{I_0(\kappa)}\right) \tag{7}$$

$$r_x''(0) = -\omega_D^2 \frac{\sigma_h^2}{2(K+1)}\left(1 + \frac{\cos(2\alpha) I_2(\kappa)}{I_0(\kappa)}\right). \tag{8}$$

Equations (6)–(8) will enable us to characterize the effect of $\boldsymbol{\psi} \neq \mathbf{0}$ on covariance-based velocity estimators in Section V.

Using the results in [16], it is also possible to see the effects of directional scattering and the LOS component on the envelope level crossing rate (LCR). The LCR is defined as the expected number of envelope crossings per second of a given level R with positive slope, and can be shown to be (see, e.g., [18]),

$$\mathrm{LCR}(R) = \int_0^\infty |\dot{R}| p_{|\dot{h}|,|h|}(\dot{R}, R)\, d\dot{R} \tag{9}$$

where $p_{|\dot{h}|,|h|}(\dot{R}, R)$ is the joint probability density function of the envelope with its time derivative. In [16], the authors showed that even in the presence of a specular component and correlated I/Q components of $x(t)$ (which is caused by $\kappa \neq 0$ in our model), the LCR of the envelope is proportional to ω_D and is entirely determined by $r_h^{(n)}(0)$, $n = 0, 1, 2$

$$\mathrm{LCR}(R, \boldsymbol{\psi}) = \frac{2R\sqrt{2\beta}}{\pi^{3/2} r_x(0)} e^{-(R^2+\rho^2)/r_x(0)} \int_0^{\pi/2} \cosh\left(\frac{2R\rho\cos\theta}{r_x(0)}\right) \times \left[e^{-(\gamma\rho\sin\theta)} + \sqrt{\pi}\gamma\rho\sin\theta\, \mathcal{Q}(\gamma\rho\sin\theta)\right] d\theta \tag{10}$$

where

R	the level;
ρ	$\lvert y(t)\rvert$ in (1) (amplitude of the specular component);
$\mathcal{Q}(\cdot p)$	the error function;
β	$-(1/2)r_x''(0) - [\mathcal{I}\{r_x'(0)\}^2/2r_x(0)]$;
γ	$[\omega_D \cos\theta_0 - \mathcal{I}\{r_x'(0)\}/r_x(0)]/\sqrt{2\beta}$.

Hence, by virtue of the fact that we have a closed-form relationship between $r_x^{(n)}(0)$, $n = 0, 1, 2$ and $\boldsymbol{\psi}$ through equations (6)–(8), we can numerically evaluate the effect of K, κ, α and θ_0 on LCR(R, $\boldsymbol{\psi}$) using (10). We will pursue this approach in the simulations and examine LCR(R, $\boldsymbol{\psi}$)/LCR(R, $\mathbf{0}$) where $\mathrm{LCR}(R, \mathbf{0}) = (\beta/2\pi)^{1/2}(R/r_x(0)) \exp[-R^2/(2r_x(0))] = (\omega_D/\sqrt{2\pi})R\exp(-R^2)$, to see how directional scattering and a LOS component affect the LCR estimator that utilizes $|h(t)|$. A parametric model for asymmetrical Doppler spectra was also adopted in [16] and the effects of the parameters on the LCR was

characterized using (10). Here, we use (10) to relate the LCR to the AOA distribution in order to compare the LCR-based velocity estimators to their covariance-based counterparts.

The model in (1) also enables us to derive the autocovariance of $|h(t)|^2$ in closed form, which is given by

$$\begin{aligned} c_{|h|^2}(\tau) &:= E[|h(t)|^2|h(t+\tau)|^2] - (E|h(t)|^2)^2 \\ &= \frac{\sigma_h^4}{(K+1)^2}\left[\left|E\left[e^{j\omega_D\cos(\theta)\tau}\right]\right|^2 + 2K\mathcal{R} \right. \\ &\quad \left. \times \left\{E\left[e^{-j\omega_D\cos(\theta)\tau}\right]e^{j\omega_D\cos(\theta_0)\tau}\right\}\right] \end{aligned} \tag{11}$$

which can be derived by using (29) in the Appendix to obtain $E[|h(t)|^2|h(t+\tau)|^2]$, and (2) to get $(E|h(t)|^2)^2$. A special case of this result was derived in [4] where $r_x(\tau)$ was assumed to be real yielding $c_{|h|^2}(\tau) = [\sigma_h^4/(K+1)^2][|E[e^{j\omega_D\cos(\theta)\tau}]|^2 + 2K[E[e^{-j\omega_D\cos(\theta)\tau}]\cos(\omega_D\cos(\theta_0)\tau)]$. Here, we extend this result to complex $r_x(\tau)$s (correlated I/Q components) which occur when the scattering is directional. Note that (11) is a straightforward consequence of (29) in the Appendix and relative to the derivation in [4], it is simpler because it does *not* make use of such complicated expressions as the joint pdf of $|h(t)|$, $|h(t+\tau)|$, $\angle h(t)$, $\angle h(t+\tau)$. One can use the closed-form expression for $r_h(\tau)$ in (4) and substitute it into (11) to explicitly see the effect of $\boldsymbol{\psi}$ on $c_{|h|^2}(\tau)$. Notice that when $K = \kappa = 0$, (11) reduces to $c_{|h|^2}(\tau) = \sigma_h^4 J_0^2(\omega_D\tau)$.

III. Novel Velocity Estimator

In this section, we propose novel velocity estimators that use $\mathcal{R}\{h(t)\}$, $\mathcal{I}\{h(t)\}$ when the I/Q components are measured or estimated, or, utilize $|h(t)|^2$, when only the channel envelope is available. It is well-known that ω_D is directly proportional to the second spectral moment, which is a measure of the Doppler bandwidth, and a decreasing function of $r_h''(0)$, the curvature of $r_h(\tau)$ at zero. This notion can be made more precise with the following:

$$\omega_D = \sqrt{\frac{-2r_h''(0)}{r_h(0)}} \tag{12}$$

which is valid when $K = \kappa = 0$, i.e., when $r_h(\tau) = \sigma_h^2 J_0(\omega_D\tau)$. Since it is often unfeasible to estimate $\boldsymbol{\psi}$ accurately, we will adopt the common strategy [3], [5] of assuming $\boldsymbol{\psi} = \mathbf{0}$ in designing our velocity estimator and subsequently deriving the effect of $\boldsymbol{\psi} \neq \mathbf{0}$ on the estimator. Our velocity estimator aims at estimating $r_h(0)$ and $r_h''(0)$ separately and uses (12) to get an estimate for ω_D. To this end, we will fit a parabola to the L points of the sample correlations $\{\hat{r}_h(lT_s)\}_{l=0}^{L}$, where T_s is the sampling period. We will assume that the sampling rate $1/T_s$ is sufficiently high to insure $LT_s \ll 1$, which is satisfied, for example, if channel samples used to estimate $r_h(0)$ and $r_h''(0)$ are provided by channel estimators of narrow band TDMA systems. The steps for estimating ω_D from the I/Q components of $h(t)$ are as follows.

Step 1) Find the correlation estimates $\{\hat{r}_h(lT_s)\}_{l=0}^{L}$ by sample averaging.

Step 2) Find $\hat{a}_k = \arg\min_{a_k}\sum_{l=0}^{L}|\hat{r}_h(lT_s) - \sum_{k=0}^{2} a_k l^k|^2$.

Step 3) Obtain $\hat{r}_h^{(n)}(0) = n!\hat{a}_n/T_s^n$, $n = 0, 2$.

Step 4) Substitute $\hat{r}_h^{(n)}(0)$, $n = 0, 2$, in (12).

Note that the mapping from the correlation estimates to the Taylor's series coefficient estimates $(\{\hat{r}_h(lT_s)\}_{l=0}^{L} \rightarrow \{\hat{r}_h^{(n)}(0)\}_{n=0}^{2})$ that solves the least squares problem in Step 2) is a linear transformation [a $3 \times (L+1)$ matrix multiplication] which can be precomputed once T_s is known. Unlike [14], to estimate ω_D we will only use a second-order polynomial, which, in view of the fact that ω_D can be estimated from $r_h^{(n)}(0)$ for $n = 0, 2$, obviates unnecessary approximations and the need for finding the roots of a higher than second-order polynomial. Notice that, in practice, Steps 1)–4) will be applied to $\mathcal{R}\{h(t)\}$ or $\mathcal{I}\{h(t)\}$, which are obtained from the in-phase and quadrature-phase components of the NB channel. In fact, it can be shown using (1) that the correlation function of $\mathcal{R}\{h(t)\}$ is given by $r_{\mathcal{R}\{h\}}(\tau) = r_h(\tau)/2$, which, in turn implies that the velocity estimator can be expressed in terms of $\mathcal{R}\{h(t)\}$ as $(-2r''_{\mathcal{R}\{h\}}(0)/r_{\mathcal{R}\{h\}}(0))^{1/2}$.

If we only have the envelope $|h(t)|$ available, we can use $|h(t)|^2$ to estimate ω_D, by exploiting the fact that $c_{|h|^2}(\tau)|_{\boldsymbol{\psi}=\mathbf{0}} = \sigma_h^4 J_0^2(\omega_D\tau)$ [cf. (11)], which can be used to show

$$\omega_D = \sqrt{\frac{-c''_{|h|^2}(0)}{c_{|h|^2}(0)}} \tag{13}$$

when $\boldsymbol{\psi} = \mathbf{0}$. Hence, to estimate ω_D from $|h(t)|^2$, we would still use steps 1)–4) except $\{\hat{c}_{|h|^2}(lT_s)\}_{l=0}^{L}$ would be estimated from $|h(t)|^2$ and $\hat{c}_{|h|^2}^{(n)}(0)$, $n = 0, 2$ would be substituted into (13) after it is computed.

IV. Relationship with Other Covariance-Based Estimators

In [11], Holtzman and Sampath proposed a covariance-based Doppler estimator using the formula

$$\hat{\omega}_D^{HS} := \frac{C}{lT_s}\sqrt{\frac{V(lT_s)}{\hat{c}_z(0)}} \tag{14}$$

where

$$V(lT_s) := \frac{1}{N}\sum_{n=0}^{N-1}[z((n+l)T_s) - z(nT_s)^2$$

$$\hat{c}_z(0) := \frac{1}{N}\sum_{n=0}^{N-1} z^2(nT_s) - \left(\frac{1}{N}\sum_{n=0}^{N-1} z(nT_s)\right)^2$$

and C is a constant depending on whether $z(t) = \mathcal{R}\{h(t)\}$, $|h(t)|^2$, or $\log|h(t)|$. Anim–Appiah has analyzed this class of covariance-based estimators in great detail in a recent paper [3], where he considered the cases $z(t) = |h(t)|^n$ and $z(t) = \mathcal{R}\{h(t)\}^n + \mathcal{I}\{h(t)\}^n$.

In order to relate the estimator in (14) to the proposed estimator, it is important to realize that $E[V(lT_s)] = 2[c_z(0) -$

$c_z(lT_s)]$, where $c_z(\tau)$ is the covariance function of $z(t)$, and recall the following result from [5]:

$$\lim_{T_s\to 0}\frac{C}{lT_s}\sqrt{\frac{E[V(lT_s)]}{c_z(0)}}=\frac{C}{l}\sqrt{\frac{-c_z''(0)}{c_z(0)}} \tag{15}$$

which is a constant multiple of (12), when $z(t)=\mathcal{R}\{h(t)\}$. The limit in (15) can be shown by substituting $2[c_z(0)-c_z(lT_s)]$ for $E[V(lT_s)]$, moving the $1/T_s$ inside the square root and applying L'Hôspital's rule twice. Equation (15) illustrates that the covariance-based estimator in [11] is affected by a $\boldsymbol{\psi}\neq\mathbf{0}$ the same way as the one proposed in Section III, when N is large and T_s is small. In the next section we derive the effect of $\boldsymbol{\psi}$ on all velocity estimators that approximate (12) or (13), which includes the proposed estimator, the estimator in [11] when $z(t)=h(t)$, or $z(t)=|h(t)|^2$, and the zero crossing rate estimator that utilizes $\mathcal{R}\{h(t)\}$ (henceforth just "ZCR").

V. Joint Effect of K and κ on $\hat{\omega}_D$

Using the expressions for $r_x^{(n)}(0)$, $n=0,\,1,\,2$ in (6)–(8) we will show that all velocity estimators under consideration that are designed for $\boldsymbol{\psi}=\mathbf{0}$, get scaled as a function of K, κ, α and θ_0, and derive the corresponding scale function $S(\boldsymbol{\psi})$. Consider first the covariance-based estimators that approximate (12). Using (2), (6), and (8) we obtain

$$\begin{aligned}\sqrt{\frac{-2r_h''(0)}{r_h(0)}}&=\omega_D\left[\frac{1}{(K+1)}\left(1+\frac{\cos(2\alpha)I_2(\kappa)}{I_0(\kappa)}\right)\right.\\&\qquad\left.+\frac{K}{K+1}\left(1+\cos(2\theta_0)\right)\right]^{1/2}\\&:=\omega_D C_1(\boldsymbol{\psi}).\end{aligned}\tag{16}$$

Notice that $C_1(\mathbf{0})=1$ as expected. Examining (16) more closely, we realize that for large values of K, the scale factor is not influenced by κ and α and depends solely on the LOS direction θ_0. An extreme case would be $\theta_0=\pi/2$ for large K, which would yield a Doppler estimate of $\hat{\omega}_D=0$. This is because $h(t)$ in (1) would not be time-dependent, a situation where the received signal contains no information about ω_D.

Remark: It is well known that for $K=0$ the ZCR estimator (of either the in-phase or quadrature component) converges to $\pi^{-1}[-r_h''(0)/r_h(0)]^{1/2}$, a fact which requires the $h(t)$ to be Gaussian [18]. Hence, for $K=0$, $h(t)$ will be Gaussian and also the ZCR estimators will be scaled by $C_1(0,\,\theta_0,\,\kappa,\,\alpha)$ in (16). On the other hand, when $K\neq 0$, if $y(t)$ is assumed to be deterministic (Aulin's model in [4]), then $h(t)$ will not be Gaussian and the expected ZCR [in the sense of (9) with the joint pdf of the in-phase component with its derivative] can be shown to be time-varying, which is not useful from a practical point of view. In order to be able to make a statement about how the ZCR estimator scales as a function of $\boldsymbol{\psi}$ when $K\neq 0$, we can argue as follows. If we assume $y(t)=Ae^{j(\omega_D\cos(\theta_0)t+\phi_0)}$ where A is a Gaussian random variable independent of $x(t)$ with $E[A]=\sigma_h[K/(K+1)]^{1/2}$ so that $E[h(t)]=\sigma_h[K/(K+1)]^{1/2}\exp[j(\omega_D\cos(\theta_0)t+\phi_0)]$ as before, then $h(t)$ will be Gaussian. This has the nice consequence that ZCR $=\pi^{-1}[-r_h''(0)/r_h(0)]^{1/2}$ even when $K\neq 0$. Under this interpretation of the model in (1), we can conclude that (16) also applies to the ZCR estimator for any value of $\boldsymbol{\psi}$.

To derive the effect of $\boldsymbol{\psi}$ on covariance-based estimators that use $|h(t)|^2$, we recall (13). Using (11) to calculate the right-hand side of (13), we see that the estimator gets scaled by a factor of $C_2(\boldsymbol{\psi})$, where it is shown in (17) at the bottom of the page. Observe that the scale factor $C_2(\mathbf{0})=1$. Note also that for $\kappa=\alpha=0$, (17) reduces to $C_2(K,\,\theta_0,\,0,\,0)=[1+K\cos(2\theta_0)/(1+2K)]^{1/2}$, which is the result derived in [11] for uniform AOA. Hence, (17) generalizes [11, eq. (6)] to when the angle of arrival distribution $p(\theta)$ is not uniform.

We reiterate here that if the LCR of $|h(t)|$ is to be used for velocity estimation, the effect of $\boldsymbol{\psi}$ given by LCR$(R,\,\boldsymbol{\psi})$/LCR$(R,\,\mathbf{0})$ can be computed numerically using (10). We will elaborate more on this in the simulation section.

VI. Estimation of the Ricean K Factor

As we mentioned before, $|h(t)|$ is a Ricean process with parameter K. It is well known that the value of K is a measure of the severity of fading with $K=0$ being the most severe Rayleigh fading, and $K=\infty$ representing no fading. Hence, the knowledge of the K factor is important in link budget calculations [8]. Also, as we have seen in the previous sections, the presence of the LOS factor introduces a modeling error in velocity estimation, which may be compensated for by estimating K. Greenwood and Hanzo in [8] have proposed techniques that fit the distribution of the envelope $|h(t)|$ to estimate K, but these techniques are not well suited for online estimation. More recently, Greenstein *et al.* introduced a moment based method for estimating K under the assumption that the LOS angle of arrival $|\theta_0|=\pi/2$ (i.e., $E[h(t)]$ is a constant) [7]. In this section, we will show that as a simple consequence of our framework, the estimator in [7] works also when $\theta_0\neq\pi/2$ [i.e., when $y(t)$ depends on time]. Consider (11) with $\tau=0$ to obtain: $c_{|h|^2}(0)=[\sigma_h^4/(K+1)^2](1+2K)$. By solving the resulting quadratic equation for K in terms of σ_h^4 and $c_{|h|^2}(0)$ we find

$$K=\frac{\sigma_h^4-c_{|h|^2}(0)+\sigma_h^2\sqrt{\sigma_h^4-c_{|h|^2}(0)}}{c_{|h|^2}(0)} \tag{18}$$

$$C_2(\boldsymbol{\psi})=\left[\frac{\left(1+\dfrac{\cos(2\alpha)I_2(\kappa)}{I_0(\kappa)}\right)-2\left(\dfrac{\cos(\alpha)I_1(\kappa)}{I_0(\kappa)}\right)^2+K\left(2+\dfrac{\cos(2\alpha)I_2(\kappa)}{I_0(\kappa)}+\cos(2\theta_0)-4\cos\theta_0\dfrac{\cos(\alpha)I_1(\kappa)}{I_0(\kappa)}\right)}{1+2K}\right]^{1/2} \tag{17}$$

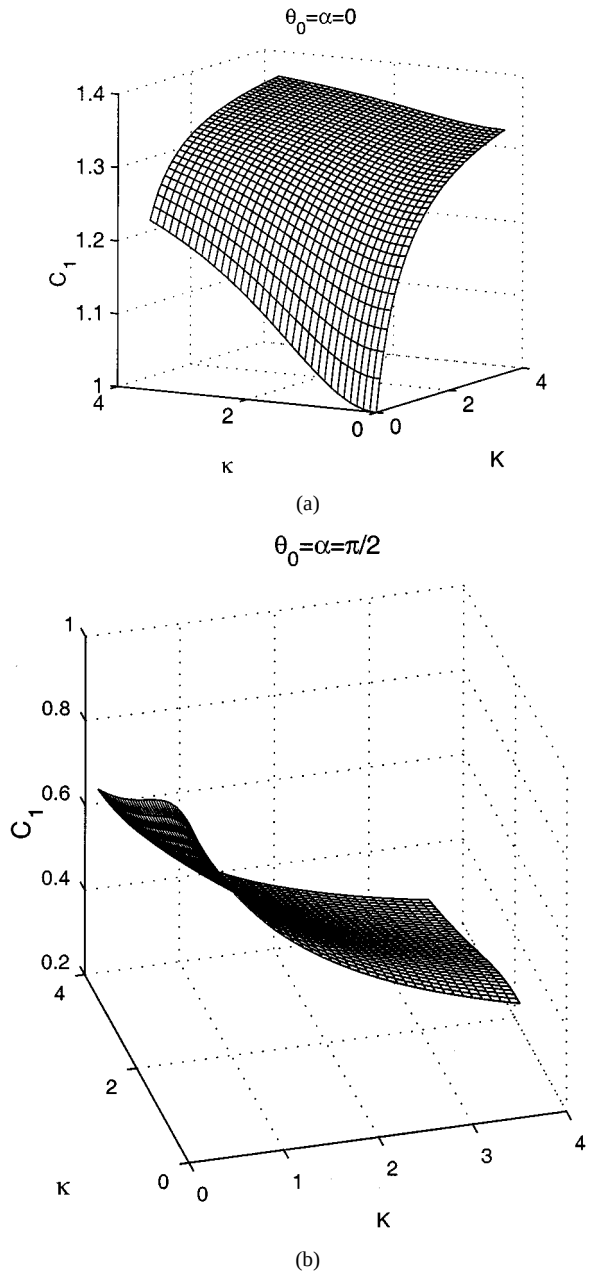

Fig. 2. (a) $C_1(\boldsymbol{\psi})$ in (16) versus κ and K, $\theta_0 = \alpha = 0$. (b) $C_1(\boldsymbol{\psi})$ in (16) versus κ and K, $\theta_0 = \alpha = \pi/2$.

which is the result in [7]. Since σ_h^4 and $c_{|h|^2}(0)$ can be estimated from $|h(t)|^2$, (18) provides us with an estimate of K. It is important to notice that $y(t)$ need not be constant for (18) to hold, as was assumed in [7].

VII. Effect of Additive White Noise

In this section, we will discuss the effect of additive white noise that is assumed to be independent of $h(t)$, on the proposed estimator and the estimator in (14) originally proposed in [11]. The effect of additive noise on velocity estimators was addressed in [5] and [11], where the noise was spectrally flat over a finite bandwidth, which results in colored noise in continuous time. We evaluate the covariance-based velocity estimators in a framework where $\hat{\omega}_D$ is estimated using noisy channel samples obtained with pilot sequences. In such a setup, if the cascade of the transmit and receive filters are designed to have Nyquist properties to avoid intersymbol interference, the channel estimates will be corrupted by uncorrelated noise in discrete time.

First, we will discuss the effect of white noise on the covariance-based estimator given in (14) when $z(nT_s) = h(nT_s) + v(nT_s)$. As mentioned in Section IV, for large N, (14) is given by

$$\hat{\omega}_D \approx \frac{C}{lT_s}\sqrt{\frac{2[c_z(0) - c_z(lT_s)]}{c_z(0)}} \tag{19}$$

which, assuming for simplicity that $h(t)$ is zero-mean and using the independence of $h(nT_s)$ and $v(nT_s)$, can be written as

$$\hat{\omega}_D \approx \frac{C}{l}\sqrt{\frac{2[r_h(0) - r_h(lT_s)]}{T_s^2[r_h(0) + r_v(0)]} + \frac{2r_v(0)}{T_s^2[r_h(0) + r_v(0)]}} \tag{20}$$

where we used the fact that $r_v(nT_s) = 0$ for $n \neq 0$. But we know that since T_s is small, we can use (15) to obtain

$$\hat{\omega}_D \approx \frac{C}{l}\sqrt{\frac{-r_h''(0)}{[r_h(0) + r_v(0)]} + \frac{2r_v(0)}{T_s^2[r_h(0) + r_v(0)]}}. \tag{21}$$

We see that if the SNR $:= r_h(0)/r_v(0)$ is moderate/low, with T_s being very small, the second term in (21) will cause $\hat{\omega}_D$ to deviate from ω_D in a pronounced manner due to the presence of noise ($r_v(0) \neq 0$). We also corroborate this in the simulations.

One way to overcome this limitation is to avoid $r_v(0)$ by adopting the following variation on ω_D^{HS} in (14):

$$\begin{aligned}\hat{\omega}_D &= \frac{1}{T_s}\sqrt{-\frac{2}{3}\frac{[V(T_s) - V(2T_s)]}{\hat{r}_z(0)}} \\ &\approx \sqrt{-\frac{2}{3}\frac{2[r_h(2T_s) - r_h(T_s)]}{T_s^2[r_h(0) + r_v(0)]}}\end{aligned} \tag{22}$$

for large N. When T_s is small, (22) yields $[-2r_h''(0)/(r_h(0) + r_v(0))]^{1/2}$, which, like (21), is also influenced by $r_v(0)$, but not nearly as much because for moderate signal-to-noise ratios (SNRs), the denominator $r_h(0) + r_v(0) \approx r_h(0)$, so $\hat{\omega}_D$ will not deviate from ω_D significantly. This "denoising" approach is similar to the one suggested in [5] for robustness against cochannel interference.

To circumvent the effect of white noise on our proposed scheme we will modify our algorithm as follows. Given noisy channel estimates $z(nT_s) = h(nT_s) + v(nT_s)$, we first obtain the estimates of $r_z(lT_s) = r_h(lT_s) + r_v(lT_s) = r_h(lT_s) + \sigma_v^2\delta_K[l]$ via sample averaging. We can then fit a polynomial to $\hat{r}_z(lT_s) \approx \hat{a}_2 l^2 + \hat{a}_0$ for $l = 1, 2, \ldots, L-1$, discarding the $l = 0$ lag to obtain estimates $\hat{r}_h''(0) = 2\hat{a}_2/T_s^2$, $\hat{r}_h(0) = \hat{a}_0$. In contrast to (22), where the noise variance affects the estimator even for large N, the proposed estimator is asymptotically unaffected by the SNR. We also illustrate this effect in the simulations.

Notice that for the aforementioned method, we do not even need to know the noise variance σ_v^2 since we can ignore the

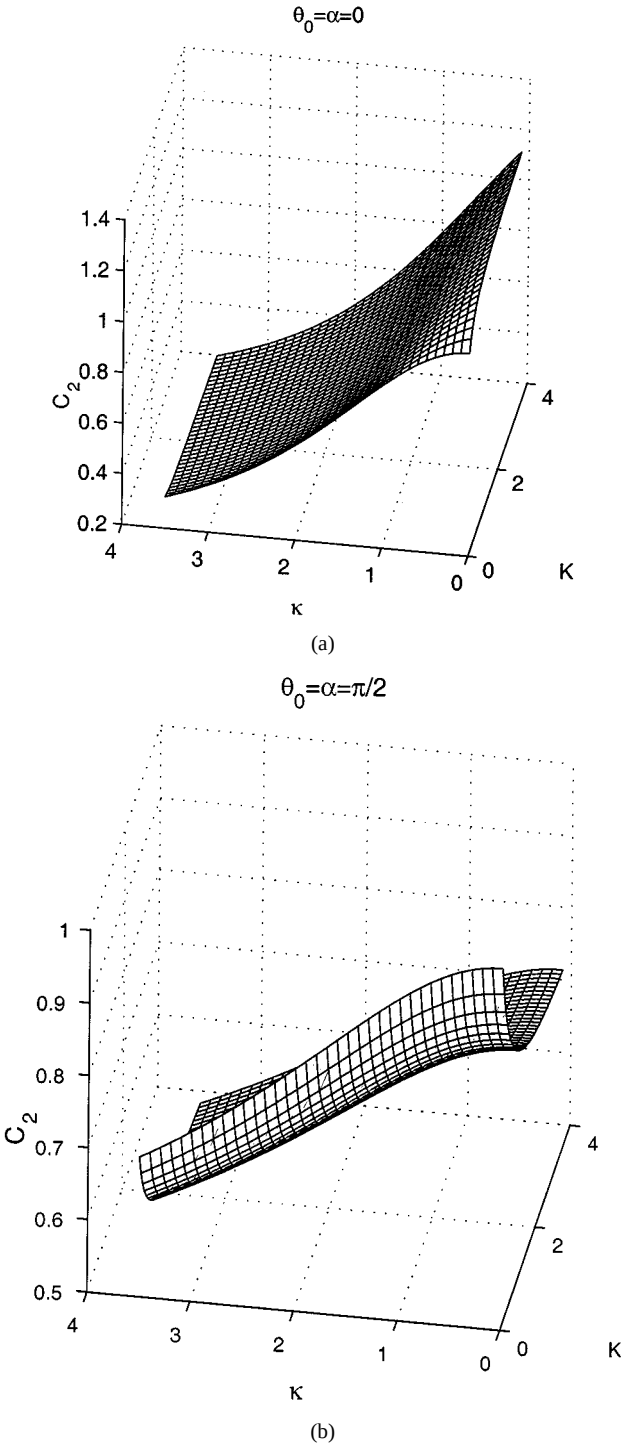

Fig. 3. (a) $C_2(\boldsymbol{\psi})$ in (17) versus κ and K, $\theta_0 = \alpha = 0$. (b) $C_2(\boldsymbol{\psi})$ in (17) versus κ and K, $\theta_0 = \alpha = \pi/2$.

white noise altogether by not using the lag $l = 0$. When the noise is colored with known color, (as might be induced with transmitter/receive filters without Nyquist properties) we can still reduce the noise effects by subtracting the noise correlation $r_v(\tau)$ from the estimate of $r_h(\tau) + r_v(\tau)$, and proceed to estimate $\hat{r}_h^{(n)}(0)$. This is a feature that $\hat{\omega}_D^{HS}$ cannot be equipped with straightforwardly since the correlations are only implicitly calculated in (14).

VIII. Simulations

In this section, we will compare the different velocity estimators designed for $\boldsymbol{\psi} = \mathbf{0}$ (i) on the basis of how sensitive they are to $\boldsymbol{\psi}$ for large N and (ii) on the basis of how fast their sample estimates converge to their ensemble values.

For part (i), in Figs. 2–4, we plotted $C_1(\boldsymbol{\psi})$ in (16), $C_2(\boldsymbol{\psi})$ in (17), and LCR(1, $\boldsymbol{\psi}$)/LCR(1, $\mathbf{0}$) as a function of K and κ, with $\sigma_h = 1$, for $\theta_0 = \alpha = 0$ and $\theta_0 = \alpha = \pi/2$. In doing so, we illustrate the joint effects of the directivity and the LOS factor on velocity estimators, unlike existing analyzes in the literature that treat these effects individually. We chose $\alpha = \theta_0$ in all plots because it is reasonable to assume that the LOS component impinges on the antenna with approximately the same angle as the directional scattering. The range $0 \le K \le 3.5, 0 \le \kappa \le 3.5$ was dictated by commonly encountered values measured from experimental data [2], [7].

We observe that in the plots involving the envelope and the envelope squared of the received signal (Figs. 3 and 4), increasing κ decreases the scale functions, whereas for Fig. 1 which is derived for the I/Q components of $h(t)$, increasing κ increases the scale factor. We also notice that in Fig. 4, for $\theta_0 = \alpha = \pi/2$ and small κ, K has little influence on the LCR. This fact was observed in [5], where only $\theta_0 = \pi/2$ (constant specular component) was considered, and was used to design a velocity estimator based on the LCR of the envelope that is robust to variations in K. We see that when $\theta_0 = 0$ and κ is small, the LCR is even less affected along values of K, which illustrates that the LCR estimator is indeed robust to variations in K. It should be noticed though, that the normalized LCR deviates from one for increasing κ especially when $\theta_0 = 0$, even though this deviation is less pronounced than that of $C_1(\boldsymbol{\psi})$ and $C_2(\boldsymbol{\psi})$ over practical parameter ranges of interest, as we will soon show.

To gain further insight into how the velocity estimators behave for arbitrary $\theta_0 = \alpha$ (not necessarily zero or $\pi/2$), we calculated the maximum and minimum values of $C_1(\boldsymbol{\psi})$, $C_2(\boldsymbol{\psi})$, and LCR(1,$\boldsymbol{\psi}$)/LCR(1,$\mathbf{0}$) over all possible $\boldsymbol{\psi} \in \mathcal{A}$ where $\mathcal{A} = \{[K,\ \theta_0,\ \kappa,\ \alpha] \in \mathbb{R}^4\colon\ 0 \le K \le 3.5,\ 0 \le \kappa \le 3.5,\ 0 \le \theta_0 = \alpha \le 2\pi\}$. In Table I, we list the maxima and minima corresponding to the scale function for each velocity estimator as well as the values of $\boldsymbol{\psi}$ that attain these optima. We also computed the RMSE $:= [\int_{\boldsymbol{\psi}\in\mathcal{A}} |S(\boldsymbol{\psi}) - 1|^2\, d\boldsymbol{\psi}]^{1/2}$ where $S(\boldsymbol{\psi})$ is $C_1(\boldsymbol{\psi})$, $C_2(\boldsymbol{\psi})$, or LCR(1, $\boldsymbol{\psi}$)/LCR(1, $\mathbf{0}$). The RMSE value quantifies the average deviation of the scale functions from their ideal value of one over $\mathcal{A}$ for each estimator. We conclude that the LCR estimator is most robust to K, κ, α and θ_0 over practical ranges of these parameters.

In the remaining figures, we generate 100 different realizations of $h(t)$ and plot the histogram for the 100 velocity estimates normalized by the true velocity, corresponding to each realization, for the given method. The performance of each estimator can be judged by how closely its histogram is clustered around one. In all experiments $v = 100$ km/h, and $T_s = 4.12 \times 10^{-5}$, which is the symbol period for the IS-54 TDMA standard adopted in North America. The carrier frequency is $f_c = 900$ MHz implying $\omega_D/2\pi \approx 83.3$ Hz. For the proposed method we chose $L = 15$ correlation lags.

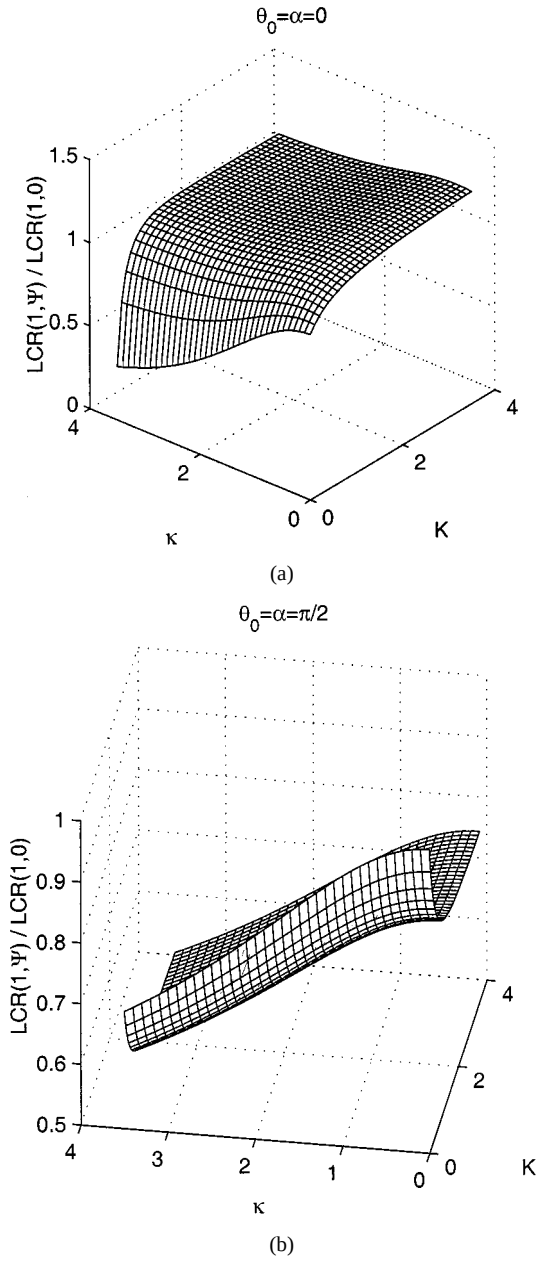

Fig. 4. (a) Deviation of LCR with K and κ, $\theta_0 = \alpha = 0$. (b) Deviation of LCR with K and κ, $\theta_0 = \alpha = \pi/2$.

TABLE I
EFFECT OF $\boldsymbol{\psi}$ ON VELOCITY ESTIMATORS

Scale	max	$\boldsymbol{\psi}_{max}$	min	$\boldsymbol{\psi}_{min}$	RMSE
C_1	1.3759	[3.5 0 3.5 0]	0.3272	[3.5 $\pi/2$ 3.5 $\pi/2$]	8.4912
C_2	1.2	[3.5 0 0 0]	0.2843	[3.5 0 3.5 0]	11.9708
LCR	1.2831	[3.5 0 0.3 0]	0.3230	[0 0 3.5 0]	6.1563

In Figs. 5–9 we simulated the finite sample behavior of the proposed estimator, $\hat{\omega}_D^{HS}$ in (14), its "denoised" version in (22), and the velocity estimator that uses the LCR of $|h(t)|$, which we will denote by $\hat{\omega}_D^{\mathrm{LCR}}$. In Figs. 5–9, all estimators not relying on the level crossings utilize $\mathcal{R}\{h(t)\}$. We generated the NB signal using the simulator in [10], which approximates Jakes's spectrum. We assumed $\boldsymbol{\psi} = \mathbf{0}$ all through, because we are interested in analyzing the finite sample behavior of the aforementioned estimators independent of any modeling error caused by $\boldsymbol{\psi} \neq \mathbf{0}$.

In Fig. 5, we observe that for a time duration of 0.02 s ($N = 485$ samples) the sample variances of the covariance-based estimators ($\hat{\omega}_D^{HS}$ and the proposed) are an order of magnitude smaller than their LCR-based counterpart, and that the proposed estimator has a slightly smaller sample variance than $\hat{\omega}_D^{HS}$. This illustrates that as far as convergence of estimators to their ensemble values is concerned, at high sampling rates and small estimation windows, covariance-based estimators are more reliable than their LCR-based counterparts. This is because, for such small data lengths, the signal does not experience many level crossings as can also be seen from the top-left plot in Fig. 5. This large gap in the maximum Doppler spread estimator variance for small window lengths between the LCR-based schemes and those that rely on the covariances, to the best of the authors' knowledge, have not been reported in the literature, and is important to know in contexts where quick estimates of $\hat{\omega}_D$ are needed, such as adaptive modulation/coding.

In Figs. 6 and 7 where we increase the time duration to 0.1 s ($N = 2427$) and 1 s ($N = 24\,271$) respectively, we observe that the covariance-based estimators still perform better than $\hat{\omega}_D^{\mathrm{LCR}}$, but the gap in the sample variances decreases as N increases, which is what we should expect if all of the estimators are consistent.

In Figs. 8 and 9 we look at the effect of white noise at SNR $= 20$ dB. We observe that $\hat{\omega}_D^{HS}$ performs very poorly as explained by (21) and among the "denoised" covariance-based estimators the proposed estimator has an order of magnitude less variance than the one in (22) in the presence of noise. In Fig. 10, we compared the proposed estimator employing $\mathcal{R}\{h(t)\}$, the proposed estimator using $|h(t)|^2$ and the modified ("denoised") estimator in (22) using $|h(t)|^2$. We see that at SNR $= 20$ dB and a data length of $N = 2427$ the estimator that employs the squared envelope has significantly better variance than the other two estimators.

In conclusion, we see that as far as the convergence of sample estimates and sensitivity to white noise is concerned, the proposed estimator (whether it uses the envelope or the I/Q components) is always the best alternative, when $T_s \ll 1$. The intuitive explanation for this is that the proposed estimator involves more correlation lags and hence it is more reliable as compared to $\hat{\omega}_D^{HS}$. Naturally, utilizing more correlation lags to improve performance comes at the expense of more computational complexity.

IX. CONCLUSION

In this paper, we proposed novel velocity estimators which are shown by the simulations to outperform the existing covariance-based, and LCR-based estimators in the sense of speed of convergence and robustness to white noise. We also showed that all the velocity estimators that are discussed get scaled as a function of $\boldsymbol{\psi}$, and derived this scale function for each estimator. We established the mean-square consistency of the sample covariances of $h(t)$ under some assumptions on $p(\theta)$ and argued that

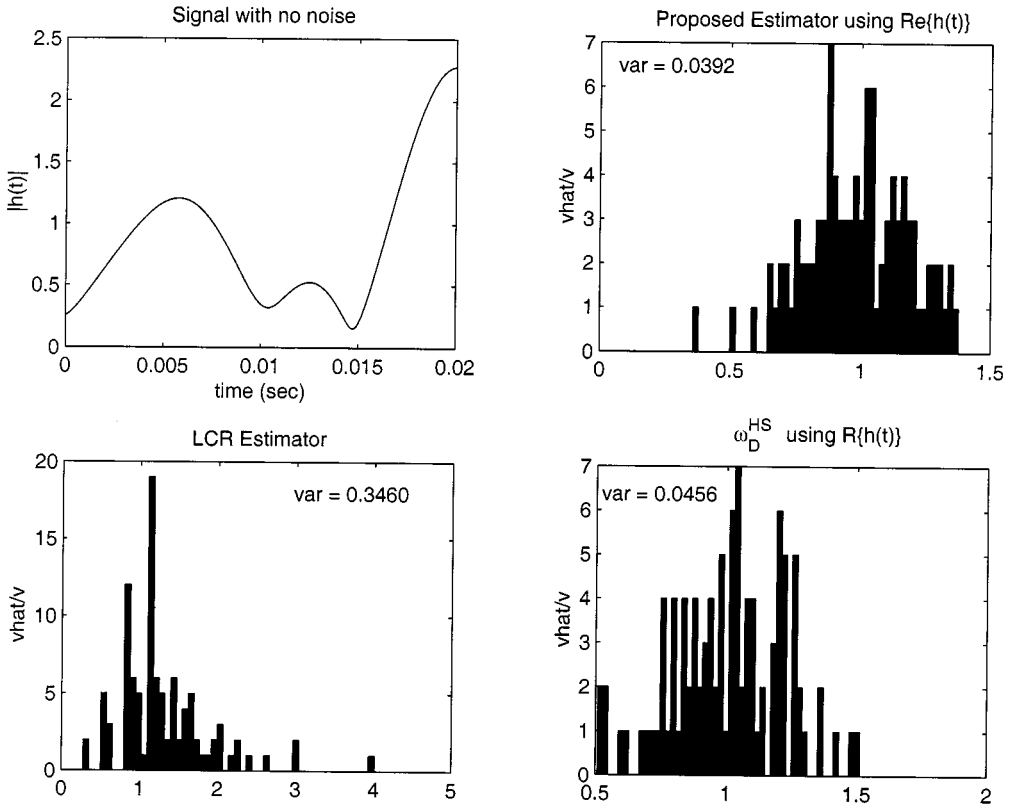

Fig. 5. Histogram of velocity estimates for $N = 485$ (0.02 s).

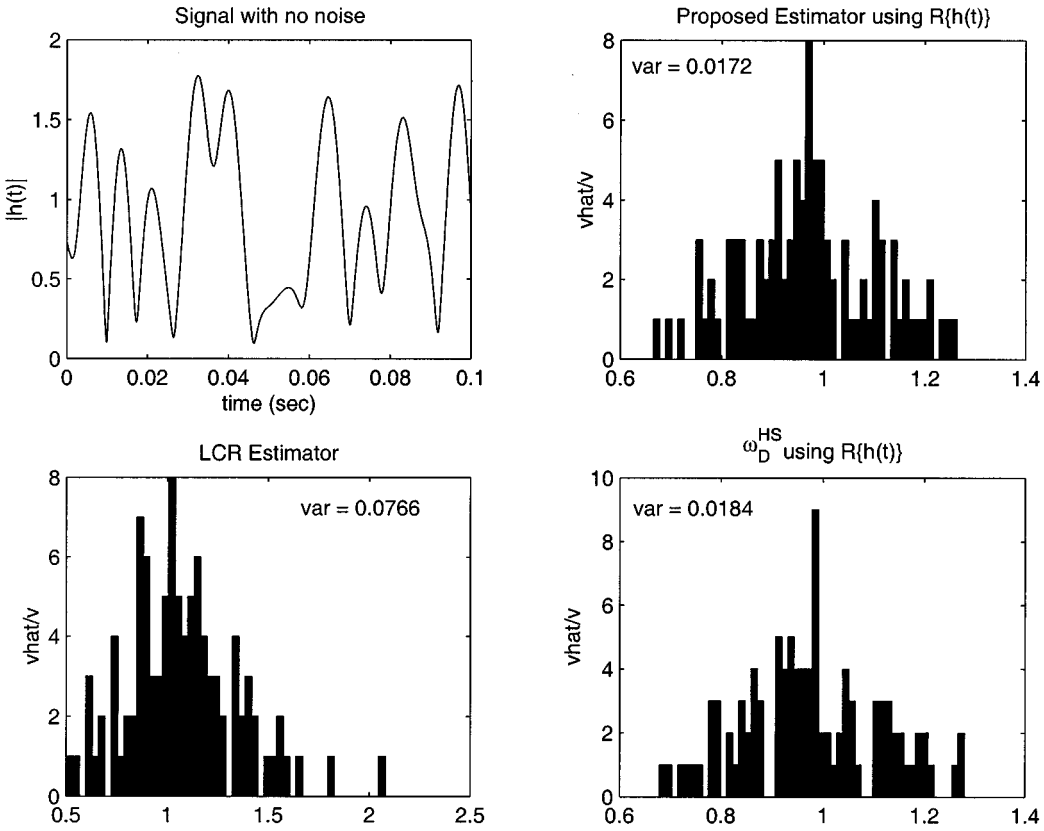

Fig. 6. Histogram of velocity estimates for $N = 2427$ (0.1 s).

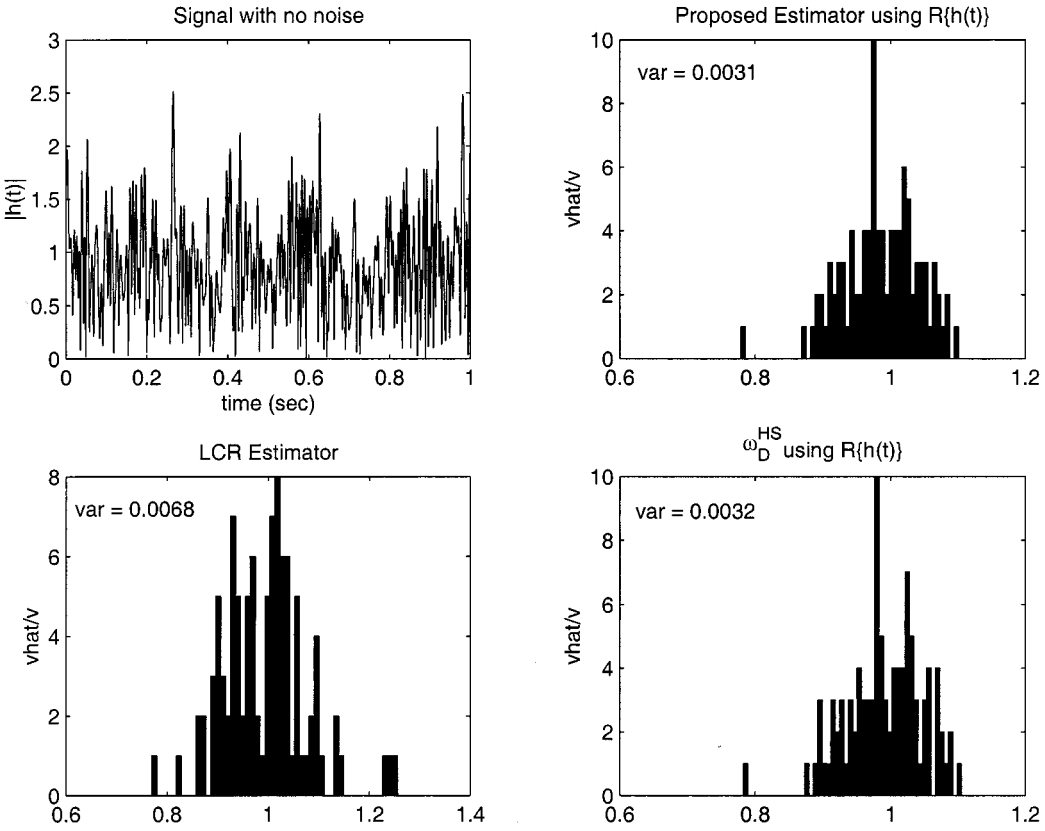

Fig. 7. Histogram of velocity estimates for $N = 24\,271$ (1 s).

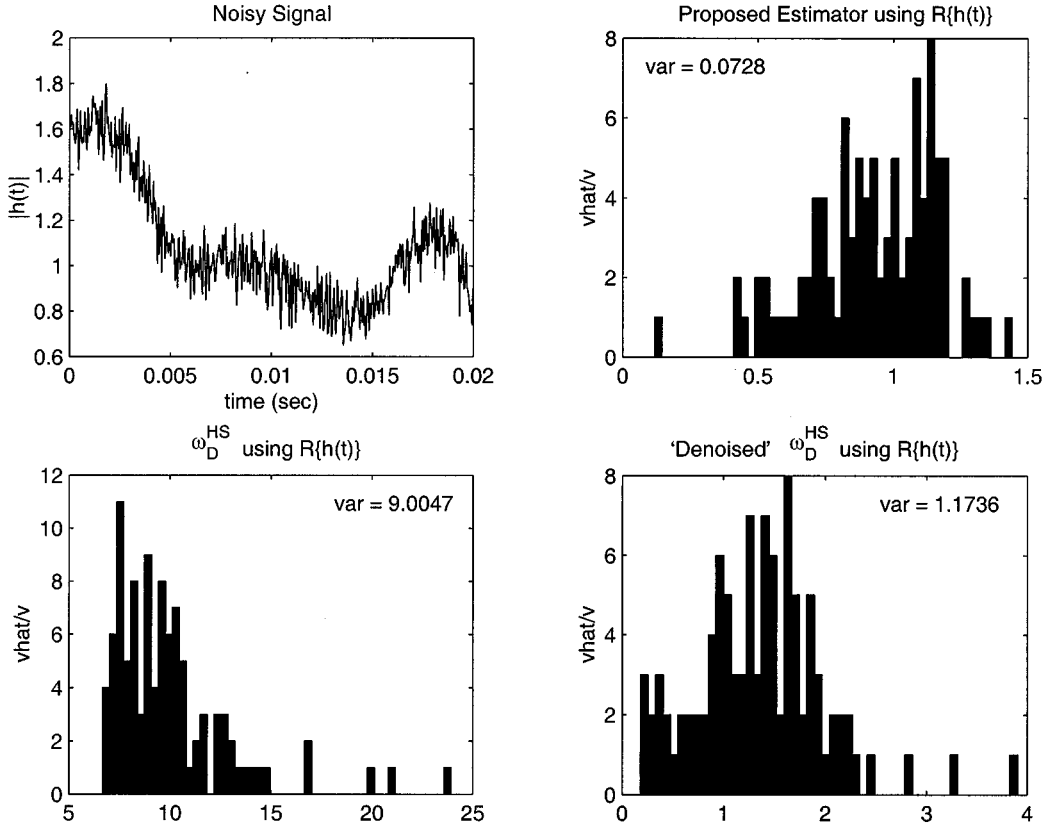

Fig. 8. Histogram of velocity estimates for $N = 485$, SNR $= 20$ dB.

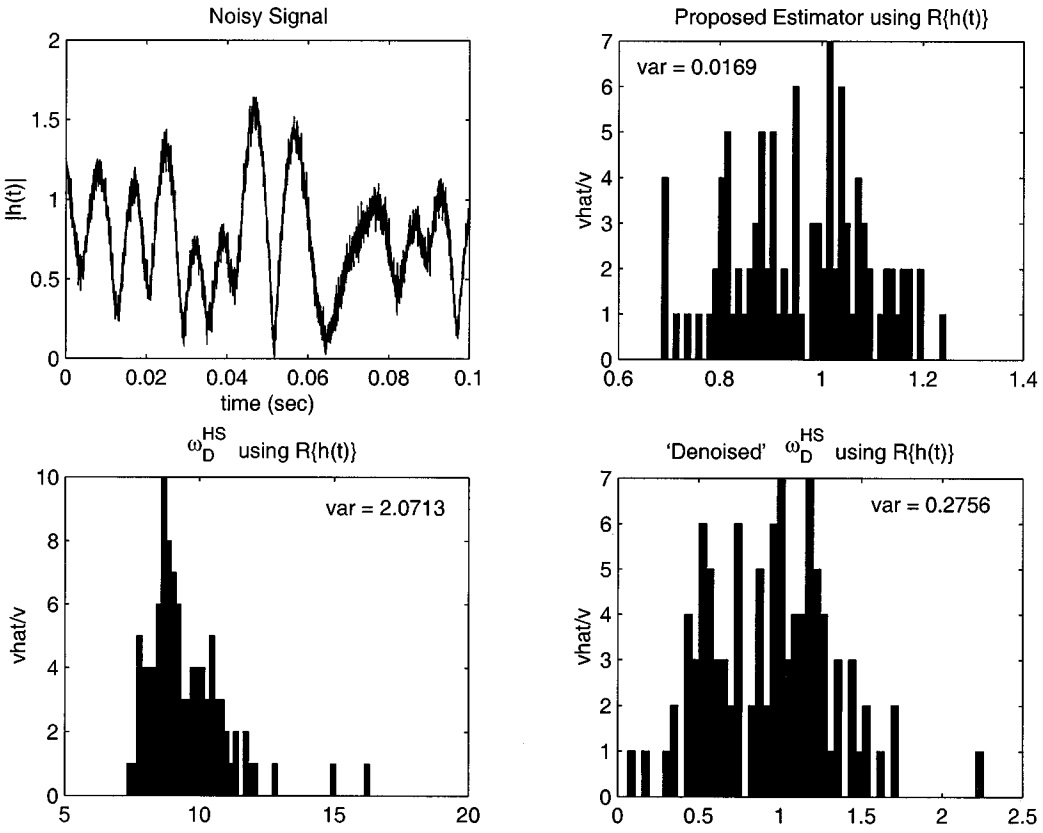

Fig. 9. Histogram of velocity estimates for $N = 2427$, SNR $= 20$ dB.

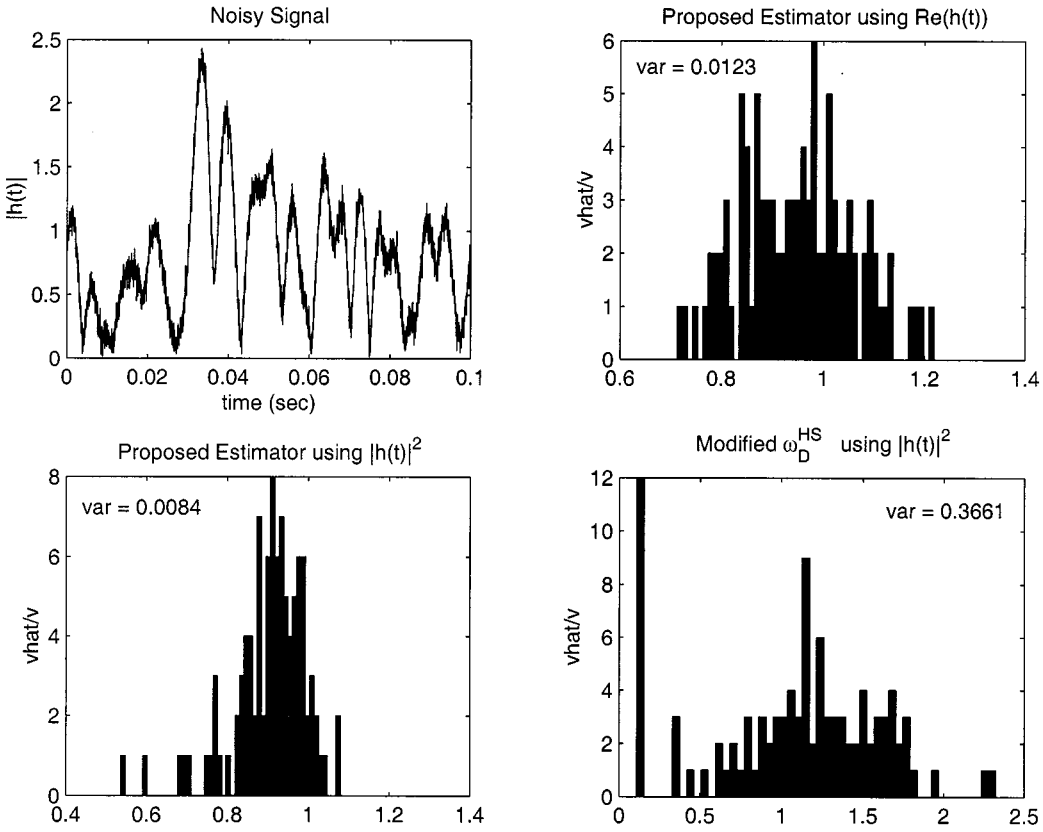

Fig. 10. Histogram of velocity estimates for $N = 2427$, SNR $= 20$ dB.

this implies the consistency of $\hat{\omega}_D^{HS}$ and of the proposed estimator utilizing $\mathcal{R}\{h(t)\}$. We saw in the process of deriving the consistency of the sample covariances of $h(t)$ that we can generalize Aulin's result [4] for the covariance of $|h(t)|^2$ to when $r_x(\tau)$ is complex, using a simpler derivation. This expression led to the verification of an estimator originally proposed [7] for the Ricean K factor that is based on moments of $|h(t)|^2$ and the recognition of the fact that this estimator is a valid one even when $y(t)$ is time variant.

APPENDIX

In this Appendix, we will show that the sample covariance of $h[n]$ in (1) converges to its ensemble value in (2), whenever the angular distribution $p(\theta)$ is bounded.[2]

Variance of the sample covariance $\hat{r}_h[l] := N^{-1}\sum_{n=0}^{N-1} h[n]h^*[n+l]$ can be expressed as

$$\begin{aligned}\mathrm{var}(\hat{r}_h[l]) = &\frac{1}{N^2}\sum_{n_1=0}^{N-1}\sum_{n_2=0}^{N-1} \\ &\times E[h[n_1]h^*[n_1+l]h^*[n_2]h[n_2+l]] \\ &- |E[\hat{r}_h[l]]|^2. \end{aligned} \tag{23}$$

We will first evaluate the expectation in the double sum using (1) after substituting $h[n] = x[n] + y[n]$. It is easy to verify the following from (1): 1) $E[x[n]] = 0$; 2) $E[x[m]x[n]] = 0, \forall m, n$ (i.e., unconjugated correlations of $x[n]$ are zero); and 3) $E[x_1[n_1]x_2[n_2]x_3[n_3]] = 0$, where $x_i[n]$ are either $x[n]$ or $x^*[n]$, which means that any expectation containing exactly three terms of $x[n]$ is zero regardless of whether any of the terms is conjugated or not. It is not surprising that 1)–3) can be shown using (1) since $x(t)$ is a Gaussian process. Using 1)–3) above, we can write

$$\begin{aligned}&E[h[n_1]h^*[n_1+l]h^*[n_2]h[n_2+l]] \\ &\quad = E[x[n_1]x^*[n_1+l]x^*[n_2]x[n_2+l]] \\ &\qquad + 2\mathcal{R}\{E[x[n_1]x^*[n_1+l]]y^*[n_2]y[n_2+l]\} \\ &\qquad + 2\mathcal{R}\{E[x^*[n_1+l]x[n_2+l]]y[n_1]y^*[n_2]\} \\ &\qquad + y[n_1]y^*[n_1+l]y^*[n_2]y[n_2+l] \\ &\quad := A_1 + A_2 + A_3 + A_4. \end{aligned} \tag{24}$$

It is straightforward to derive the last three terms as

$$\begin{aligned}&A_2 + A_3 + A_4 \\ &\quad = \frac{\sigma^4 K}{(K+1)^2}\, 2\mathcal{R}\left\{E\left[e^{-j\omega_D\cos(\theta)l}\right] e^{j\omega_D\cos(\theta_0)l}\right\} \\ &\qquad + \frac{\sigma^4 K}{(K+1)^2}\, 2\mathcal{R}\left\{E\left[e^{-j\omega_D\cos(\theta)(n_1-n_2)}\right]\right. \\ &\qquad \left.\times e^{j\omega_D\cos(\theta_0)(n_1-n_2)}\right\} + \frac{\sigma^4 K^2}{(K+1)^2}. \end{aligned} \tag{25}$$

The computation of the first term A_1 is more involved. Since ϕ_m are uniformly distributed $E[\exp[j(\phi_{m_1} - \phi_{m_2} - \phi_{m_3} + \phi_{m_4})]] = \delta_{m_1,m_2}\delta_{m_3,m_4} + \delta_{m_1,m_3}\delta_{m_2,m_4} - \delta_{m_1,m_2}\delta_{m_3,m_4}\delta_{m_1,m_3}$ [17, p. 168], where $\delta_{i,j} := \delta_K[i-j]$ for compact notation. Then A_1 is given by

$$\begin{aligned}A_1 = &\frac{\sigma_h^4}{(K+1)^2}\lim_{M\to\infty}\frac{1}{M^2}\sum_{m_1,m_2,m_3,m_4=1}^{M} a_{m_1}a_{m_2}^*a_{m_3}^*a_{m_4} \\ &\times E\left[\exp\left(j\omega_D[\cos(\theta_{m_1})n_1 - \cos(\theta_{m_2})(n_1+l)\right.\right. \\ &\left.\left. - \cos(\theta_{m_3})n_2 + \cos(\theta_{m_4})(n_2+l)]\right)\right] \\ &\times [\delta_{m_1,m_2}\delta_{m_3,m_4} + \delta_{m_1,m_3}\delta_{m_2,m_4} \\ &\quad - \delta_{m_1,m_2}\delta_{m_3,m_4}\delta_{m_1,m_3}] \end{aligned} \tag{26}$$

which can be reduced to

$$\begin{aligned}A_1 = &\frac{\sigma_h^4}{(K+1)^2}\lim_{M\to\infty}\frac{1}{M^2} \\ &\times\left[\sum_{m=1}^{M}|a_m|^4 + \left(\sum_{m_1,m_2=1}^{M}|a_{m_1}|^2|a_{m_2}|^2 - \sum_{m=1}^{M}|a_m|^4\right)\right. \\ &\left.\times\left(\left|E\left[e^{j\omega_D\cos(\theta)l}\right]\right|^2 + \left|E\left[e^{j\omega_D\cos(\theta)(n_1-n_2)}\right]\right|^2\right)\right]. \end{aligned} \tag{27}$$

But since the amplitudes a_m satisfy $\lim_{M\to\infty} M^{-1}\sum_{m=1}^{M}|a_m|^2 = 1$, it follows that $\lim_{M\to\infty} M^{-2}\sum_{m=1}^{M}|a_m|^4 = 0$. Hence, (26) is given by

$$\begin{aligned}A_1 = &\frac{\sigma_h^4}{(K+1)^2}\left[\left|E\left[e^{j\omega_D\cos(\theta)l}\right]\right|^2\right. \\ &\left. + \left|E\left[e^{j\omega_D\cos(\theta)(n_1-n_2)}\right]\right|^2\right]. \end{aligned} \tag{28}$$

Combining (25) and (28), (24) can be written as

$$\begin{aligned}&E[h[n_1]h^*[n_1+l]h^*[n_2]h[n_2+l]] \\ &\quad = \frac{\sigma_h^4}{(K+1)^2}\left[\left|E\left[e^{j\omega_D\cos(\theta)l}\right]\right|^2 + \left|E\left[e^{j\omega_D\cos(\theta)(n_1-n_2)}\right]\right|^2\right] \\ &\qquad + \frac{\sigma_h^4 K}{(K+1)^2}\left[2\mathcal{R}\left\{E\left[e^{-j\omega_D\cos(\theta)l}\right]e^{j\omega_D\cos(\theta_0)l}\right\}\right. \\ &\qquad \left. + 2\mathcal{R}\left\{E\left[e^{-j\omega_D\cos(\theta)(n_1-n_2)}\right]e^{j\omega_D\cos(\theta_0)(n_1-n_2)}\right\}\right] \\ &\qquad + \frac{\sigma_h^4 K^2}{(K+1)^2}. \end{aligned} \tag{29}$$

In order to compute (23), we use (2) and (29) to obtain

$$\begin{aligned}&\mathrm{var}(\hat{r}_h[l]) \\ &\quad = \frac{1}{N^2}\frac{\sigma_h^4}{(K+1)^2}\sum_{n_1=0}^{N-1}\sum_{n_2=0}^{N-1} \\ &\qquad \times\left[\left|E\left[e^{j\omega_D\cos(\theta)(n_1-n_2)}\right]\right|^2 + 2K\mathcal{R}\right. \\ &\qquad \left.\times\left\{E\left[e^{j\omega_D\cos(\theta)(n_1-n_2)}\right]e^{-j\omega_D\cos(\theta_0)(n_1-n_2)}\right\}\right]. \end{aligned} \tag{30}$$

[2]We will adopt the convention that if $f(t)$ is a function of a continuous variable, $f[n] := f(nT_s)$ denotes a sequence consisting of its T_s-spaced samples.

Reducing the double sum in (30) into a single sum, the variance of the covariance estimator can finally be expressed as

$$\begin{aligned}\mathrm{var}(\hat{r}_h[l]) = \frac{2\sigma_h^4}{(K+1)^2}\,\frac{1}{N^2}\sum_{k=0}^{N-1}(N-k) \\ \times\left[\left|E\left[e^{j\omega_D\cos(\theta)k}\right]\right|^2 + 2K\mathcal{R}\right. \\ \left.\times\left\{E\left[e^{j\omega_D\cos(\theta)k}\right]e^{-j\omega_D\cos(\theta_0)k}\right\}\right] \\ -\frac{\sigma_h^4}{(K+1)^2}\,\frac{(1+2K)}{N}. \qquad (31)\end{aligned}$$

Clearly, $\mathrm{var}(\hat{r}_h[l])$ depends on the covariance of $x[n]$, which, in turn, depends on the angle of arrival distribution $p(\theta)$ through (2). Since the last term in (31) goes to zero as $N \to \infty$, we will concentrate on the sum in (31). Interchanging the expectation integral with the sum we obtain

$$\begin{aligned}\lim_{N\to\infty}\mathrm{var}(\hat{r}_h[l]) \\ = \lim_{N\to\infty}\frac{2\sigma_h^4}{(K+1)^2}\int_{-\pi}^{\pi}\int_{-\pi}^{\pi}p(\theta_1)p(\theta_2) \\ \times\sum_{k=0}^{N-1}\frac{N-k}{N^2}\,e^{j\omega_D k(\cos\theta_1-\cos\theta_2)}\,d\theta_1\,d\theta_2 + \lim_{N\to\infty}2K\mathcal{R} \\ \times\left\{\int_{-\pi}^{\pi}p(\theta)\sum_{k=0}^{N-1}\frac{N-k}{N^2}\,e^{j\omega_D k(\cos\theta-\cos\theta_0)}\,d\theta\right\}. \qquad (32)\end{aligned}$$

But it is well known [17] that the sum in the first term in (32) converges to zero as $N \to \infty$ except on a set of measure zero: $\{(\theta_1, \theta_2)\colon \cos\theta_1 = \cos\theta_2\}$. Hence, if $p(\theta)$ is bounded, the first term in (32) goes to zero as $N \to \infty$, and a similar argument holds for the second term. This proves the mean-square consistency of $\hat{r}_h[l]$.

Remarks:

1) Notice that when the AOA distribution is uniform (Jakes's model), $\hat{r}_h[l]$ is consistent.
2) Since $\hat{r}_h[0]$ converges to a nonzero random variable in the mean-square sense, we conclude that $\hat{\omega}_D^{HS}$ and the proposed estimator are continuous functions of the sample correlations and, hence, they are mean-square consistent as well.
3) If $p(\theta) = \sum_{i=1}^{S}\alpha_i\delta_D(\theta-\beta_i)$, yielding a finite number S of *distinct* frequencies in (1), $p(\theta)$ is not bounded. In this case, the first term in (31) does not go to zero as $N \to \infty$, implying that the sample autocorrelation is *not* mean-square consistent, agreeing with [9, p. 210], which asserts that the sample autocovariance for a Gaussian process is inconsistent whenever the discrete spectrum is present. This also illustrates that the consistency result obtained in this Appendix is not entirely academic and that the sample correlations are not consistent in all situations of practical interest.

REFERENCES

[1] A. Abdi and M. Kaveh, "A new velocity estimator for cellular systems based on higher order crossings," in *Proc. 32nd Asilomar Conf. Signals, Systems, and Computers*, Pacific Grove, CA, Nov. 1–4, 1998, pp. 1423–1427.

[2] A. Abdi, H. A. Barger, and M. Kaveh, "A parametric model for the distribution of the angle of arrival and the associated correlation function and power spectrum at the mobile station," IEEE Trans. Veh. Technol., submitted for publication.

[3] K. D. Anim-Appiah, "On generalized covariance-based velocity estimation," *IEEE Trans. Veh. Technol.*, vol. 48, pp. 1546–1557, Sept. 1999.

[4] T. Aulin, "A modified model for the fading signal at a mobile radio channel," *IEEE Trans. Veh. Technol.*, vol. 28, pp. 182–203, Aug. VT-1979.

[5] M. D. Austin and G. L. Stüber, "Velocity adaptive handoff algorithms for microcellular systems," *IEEE Trans. Veh. Technol.*, vol. 43, pp. 549–561, Aug. 1994.

[6] M. J. Chu and W. E. Stark, "Effect of mobile velocity on communications in fading channels," *IEEE Trans. Veh. Technol.*, vol. 49, pp. 202–210, Jan. 2000.

[7] L. J. Greenstein, D. G. Michelson, and V. Erceg, "Moment-method estimation of the Ricean K-factor," *IEEE Commun. Lett.*, vol. 3, pp. 175–176, June 1999.

[8] D. Greenwood and L. Hanzo, "Characterization of mobile radio channels," in *Mobile Radio Communications*, R. Steele, Ed. London, U.K.: Pentech, 1992, pp. 163–185.

[9] E. J. Hannan, *Multiple Time Series*. New York: Wiley, 1970.

[10] P. Höher, "A statistical discrete-time model for the WSSUS multipath channel," *IEEE Trans. Veh. Technol.*, vol. 41, pp. 461–468, Nov. 1992.

[11] J. M. Holtzman and A. Sampath, "Adaptive averaging methodology for handoffs in cellular systems," *IEEE Trans. Veh. Technol.*, vol. 44, pp. 59–66, Feb. 1995.

[12] S. Hu, T. Eyceöz, A. Duel-Hallen, and H. Hallen, "Transmitter antenna diversity and adaptive signaling using long range prediction for fast fading DS/CDMA mobile radio channels," in *Proc. WCNC '99*, vol. 2, New Orleans, LA, 1999, pp. 824–828.

[13] W. C. Jakes, *Microwave Mobile Communications*. New York: IEEE Press, 1974.

[14] J. Lin and J. G. Proakis, "A parametric method for Doppler spectrum estimation in mobile radio channels," in *Proc. 27th CISS*. Baltimore, MD, Mar. 1993, pp. 875–880.

[15] K. V. Mardia, *Statistics of Directional Data*. New York: Academic, 1972.

[16] M. Pätzold, U. Killat, and F. Laue, "An extended Suzuki model for land mobile satellite channels and its statistical properties," *IEEE Trans. Veh. Technol.*, vol. 47, pp. 617–630, May 1998.

[17] P. Stoica and R. Moses, *Introduction to Spectral Analysis*. Englewood Cliffs, NJ: Prentice-Hall, 1997.

[18] G. L. Stüber, *Principles of Mobile Communication*. Norwell, MA: Kluwer, 1996.

[19] V. I. Tikhonov, "The effects of noise on phase-lock oscillation operation," *Automat. i Telemekhanika*, vol. 22, no. 9, 1959.

Cihan Tepedelenlioğlu was born in Ankara, Turkey, in 1973. He received the B.S. degree (highest honors) from Florida Institute of Technology, Melbourne, in 1995 and the M.S. degree from the University of Virginia, Charlottesville, in 1998, both in electrical engineering. He is currently working toward the Ph.D. degree from the University of Minnesota, Minneapolis, in the Department of Electrical and Computer Engineering.

Since January 1999, he has been working as a Research Assistant at the University of Minnesota, His research interests include statistical signal processing, system identification, time-varying systems, and modeling, tracking, and equalization of fading channels in mobile communications.

Georgios B. Giannakis (S'84–M'86–SM'91–F'97) received the Diploma in electrical engineering from the National Technical University of Athens, Greece, 1981, the M.Sc. degrees in electrical engineering and mathematics, in 1983 and 1986, respectively, and the Ph.D. degree in electrical engineering, in 1986, all from the University of Southern California (USC), Los Angeles.

After lecturing for one year at USC, he joined the University of Virginia, Charlottelville, in 1987, where he became a Professor of electrical engineering in 1997. Since 1999, he has been with the University of Minnesota, Minneapolis, as a Professor of electrical and computer engineering. He is a frequent consultant for the telecommunications industry. His general interests span the areas of communications and signal processing, estimation and detection theory, time-series analysis, and system identification—subjects on which he has published more than 120 journal papers, 250 conference papers and two edited books. Current research topics focus on transmitter and receiver diversity techniques for single- and multi-user fading communication channels, redundant precoding and space-time coding for block transmissions, multicarrier, and wide-band wireless communication systems.

Dr. Giannakis has received three Best Paper Awards form the IEEE Signal Processing (SP) Society (1992, 1998, 2000) and the Society's Technical Achievement Award in 2000. He coorganized three IEEE-SP Workshops (OHS–1993, SAP–1996, and SPAWN–1997) and guest (co)edited four special issues. He has served as an Associate Editor for the IEEE TRANSACTIONS ON SIGNAL PROCESSING and the IEEE SIGNAL PROCESSING LETTERS. He was a secretary of the SP Conference Board, a member of the SP Publications Board and a member and vice-chair of the Statistical Signal and Array Processing Committee. He is a member of the Editorial Board for the PROCEEDINGS OF THE IEEE, he chairs the SP for Communications Technical Committee and serves as the Editor-in-Chief for the IEEE SIGNAL PROCESSING LETTERS. He is a member of the IEEE Fellows Election Committee and the IEEE-SP Society's Board of Governors.